Kinetics of Electron Transfer from Q_A to Q_B in Photosystem II†

Rik de Wijn and Hans J. van Gorkom*

Department of Biophysics, Leiden University, P.O. Box 9504, 2300 RA Leiden, The Netherlands

Received April 26, 2001; Revised Manuscript Received July 26, 2001

ABSTRACT: The oxidation kinetics of the reduced photosystem II electron acceptor Q_A^- was investigated by measurement of the chlorophyll fluorescence yield transients on illumination of dark-adapted spinach chloroplasts by a series of saturating flashes. Q_A^- oxidation depends on the occupancy of the "Q_B binding site", where this reaction reduces plastoquinone to plastoquinol in two successive photoreactions. The intermediate, one-electron-reduced plastosemiquinone anion Q_B^- remains tightly bound, and its reduction by Q_A^- may proceed with simple first-order kinetics. The next photoreaction, in contrast, may find the Q_B binding site occupied by a plastoquinone, a plastoquinol, or neither of the two, resulting in heterogeneous Q_A^- oxidation kinetics. The assumption of monophasic Q_B^- reduction kinetics is shown to allow unambiguous decomposition of the observed multiphasic Q_A^- oxidation. At pH 6.5 the time constant for Q_A^- oxidation was found to be 0.2−0.4 ms with Q_B in the site, 0.6−0.8 ms with Q_B^- in the site, 2−3 ms when the site is empty and Q_B has to bind first, and of the order of 0.1 s if the site is temporarily blocked by the presence of Q_BH_2 or other low-affinity inhibitors such as carbonyl cyanide *m*-chlorophenylhydrazone (CCCP). Effects of pH and H_2O/D_2O exchange were found to be remarkably nonspecific. No influence of the S-states could be demonstrated.

Photosystem II (PS II)[1] utilizes light-driven one-electron redox chemistry to bring about the four-electron oxidation of water to oxygen and the two-electron reduction of plastoquinone to plastoquinol (*1*). In a fraction of a nanosecond after the absorption of a photon an electron is transferred from the excited primary donor chlorophyll P_{680}, via a pheophytin molecule, to a permanently bound plastoquinone molecule, Q_A. At the donor side of the PS II reaction center (RC) P_{680}^+ oxidizes the tyrosine residue Y_Z in a multiphasic process with time constants ranging from tens of nanoseconds to tens of microseconds (*2*, *3*). Y_Z^{ox} in turn oxidizes the four-manganese cluster at the PS II donor side. In four successive charge separations the complex accumulates the four oxidizing equivalents needed to split two water molecules into protons and molecular oxygen. As a result, the complex cycles through its five so-called S-states: $S_0 \rightarrow S_1 \rightarrow S_2 \rightarrow S_3 \rightarrow S_4$, where the subscript indicates the number of oxidizing equivalents stored. The state S_4 spontaneously reverts to S_0 by water oxidation.

On the PS II electron acceptor side (*4*), which is similar to that of the better known RC of purple bacteria (*5*, *6*), electron transfer from Q_A^- to the pool of free plastoquinone molecules in the membrane requires binding of a plastoquinone molecule at the Q_B site. Q_B acts as a two-electron gate (*7*, *8*). Its semiquinone form Q_B^- is stabilized by the protein and remains tightly bound, until the next photoreaction allows its full reduction and protonation to the plastoquinol form Q_BH_2 that may be exchanged for a new plastoquinone molecule (*9*, *10*). On illumination of a dark-adapted sample by a series of single-turnover flashes, the two-electron gate causes a binary oscillation with a flash number of electron-transfer reactions at the acceptor side, superimposed on the period four oscillation due to the four-electron gate at the donor side. Since the state S_1Q_B accumulates during dark adaptation, the sequence of states produced by the first four flashes is predominantly as follows:

$$S_1Q_B \rightarrow S_2Q_B^- \rightarrow S_3Q_B \rightarrow S_0Q_B^- \rightarrow S_1Q_B$$

Although "misses" due to failure or recombination of the charge separation cause a damping of the oscillations, they affect both sides, and in each RC the correlation between S-states and Q_B-states is normally preserved throughout a flash series (*11*).

The oxidation of Q_A^- by Q_B and that by Q_B^- may have quite different properties and may also depend on the S-state. In purple bacteria Q_B has been shown to bind at a more distal position than Q_B^-, and its reduction is rate-limited by the shift to the more proximal position (*12*). The reduction of Q_B^-, on the other hand, was shown to depend on the driving force and requires prior protonation, although the latter was found to be not rate-limiting in the purple bacterial RC (*5*, *6*). In PS II the study of these reactions has been seriously hampered by the multitude of states of the RC, by PS II heterogeneity, and by malfunctioning of the two-electron gate in all but the most intact PS II preparations. Fortunately, the chlorophyll fluorescence yield in PS II provides a very

† This research was supported by the section of Chemical Sciences of The Netherlands Organization for Scientific Research (NWO-CW).

* Corresponding author. Telephone: ++31 71 5275969. Fax: ++31 71 5275819. E-mail: vanGorkom@Biophys.LeidenUniv.NL.

[1] Abbreviations: CCCP, carbonyl cyanide *m*-chlorophenylhydrazone; D (^{2}H), deuterium; DCMU, 3-(3′,4′-dichlorophenyl)-1,1-dimethylurea; EL, electroluminescence; FCCP, carbonyl cyanide *p*-(trifluoromethoxy)-phenylhydrazone; P_{680}, primary electron donor of PS II; PS II, photosystem II; Q_A, permanently bound plastoquinone, secondary electon acceptor; Q_B, exchangeable plastoquinone acting as a two-electron gate; RC, reaction center; TPB, tetraphenylboron; Y_Z, D1-tyrosine 161, secondary electron donor.

10.1021/bi010852r CCC: $20.00
Published on Web 09/08/2001

sensitive, albeit nonlinear, measure of the oxidation state of Q_A which can be used even in intact organisms (*13*). Using whole chloroplasts, the group of Crofts has studied the Q_A^- oxidation kinetics this way in relation to the two-electron gate. The fluorescence yield decay was much faster after one than after two flashes, and the fluorescence yield at a fixed (submillisecond) time after the flash showed a small but obvious binary oscillation with flash number (*14*).

In our recent study on the slow phases of P_{680}^+ reduction in osmotically swollen thylakoids (*15*), we also used measurements of fluorescence yield changes to determine the Q_A^- oxidation kinetics. Like Putrenko et al. (*16*), we confirmed the faster decay on the first flash but could not confirm the proposed Q_B/Q_B^- dependence of the oxidation rate constant (*14*). Instead, the period two oscillation of the fluorescence yield decay appeared to be largely due to the Q_B/Q_B^- dependence of the amplitude of a slow phase in Q_B reduction, often attributed to PS II centers where the Q_B site was empty at the moment of the flash. Also, the effect of exchanging H_2O with D_2O on both Q_A^- oxidation phases appeared to depend on the reduction state of Q_B, but the results were not conclusive on this point.

Prompted by these observations, we have reinvestigated the kinetics of Q_A^- oxidation as reflected in the decay of the flash-induced fluorescence yield increase upon illumination of dark-adapted spinach chloroplasts by a series of single-turnover flashes. An unambiguous separation could be obtained of the Q_A^- oxidation kinetics in PS II centers with Q_B^-, with Q_B, and with an empty Q_B site, and the effects of S-state, pH, and H_2O/D_2O exchange on each of these reactions were investigated.

MATERIALS AND METHODS

Measurements were performed on thylakoids isolated from laboratory-grown spinach leaves, essentially according to ref *17*. Shortly before measurement the thylakoids were diluted from a concentrated suspension in a buffer containing 0.4 M sucrose, 15 mM NaCl, 5 mM $MgCl_2$, and 25 mM MES/NaOH for pH values up to 6.5 or HEPES/HCl or Tricine/NaOH for higher pH. For measurement of the H/D exchange effect the thylakoids were diluted in the same buffer solution but prepared in D_2O; the pD was set using a correction for a glass electrode in D_2O according to ref *18*. Before measurement the sample was dark adapted for 15 min. Osmotically swollen chloroplasts (blebs) were formed by diluting a thylakoid suspension of 1.5 mg/mL 400-fold in a solution containing 1 mM MOPS buffer, pH = 6.6, and 1 mM $CaCl_2$. All measurements were performed at room temperature.

When applicable, FCCP, CCCP (Sigma), or DCMU (Lancaster) was added from a stock solution in ethanol. The final ethanol concentration in the sample was 0.1% or less, except for the measurement of fluorescence changes induced by addition of these chemicals (see below), where the final concentration was 1%. TPB (Sigma) was added from a stock solution in water.

For both fluorescence and electroluminescence measurements the frequency-doubled pulse (fwhm ~10 ns) of a Nd:YAG laser was used for saturating flash excitation. Emitted light was detected by a photomultiplier tube (EMI 9816A) that was shut off during the flash by an electronic gate (*19*).

Flash-Induced Fluorescence Kinetics. Fluorescence measurements were performed using the emission of blue LED's (Marl, 470 nm) filtered by a Corning 4-96 as a nonactinic excitation source. The induced fluorescence was detected through Schott KV 550 and RG 630 cutoff filters and a Balzers 686 nm interference filter. The LED's were modulated by pulsing a home-built current driver at 2 MHz. Pulse trains of the desired length could be obtained by gating the current driver with a TTL pulse. The fluorescence signal was demodulated by a 2 MHz lock-in amplifier. Artifacts resulting from the PMT gating were suppressed by simultaneously gating the input of the amplifier using a fast MOSFET. The output of the lock-in amplifier was led into an ADC that was interfaced to a PC for data storage. The instrument response time was determined by the adjustable time constant of the lock-in amplifier and was 2−3 μs minimally. By use of modulated rather than continuous measuring light, lower (less actinic) light intensities could be used, and a contribution by long-lived luminescence emission induced by the actinic flashes (PS II delayed fluorescence) was suppressed.

Measurement of flash-induced fluorescence yield changes was performed on three different time scales by using LED pulse trains of either 0.18, 1.6, or 10 ms duration. For the two shortest time scales the signals were measured at each flash of a series of consecutive laser flashes. For each flash series a fresh dark-adapted sample was taken. For the 0.18 ms measurements the 2−3 μs response time (500 kHz sampling rate) was used; for the 1.6 ms measurements the time constant was set to 10 μs (100 kHz sampling rate). To avoid double hits due to the actinic effect of the measuring light, the 10 ms measurements were performed only at the last flash of a series of 1−5 laser flashes. For each measurement a fresh dark-adapted sample was taken. A 30 μs time constant in combination with a 20 kHz sampling rate was used.

Fluorescence Changes Induced by the Addition of Chemicals. For these experiments the emission of a blue LED (as above) was used. The thylakoids were suspended at a chlorophyll concentration of 15 μg/mL in the sucrose buffer at pH = 6.5. The 1 mm path-length cuvette was placed in a special housing that allowed the addition of chemicals in the dark.

Electroluminescence. Electroluminescence (EL) measurements were performed on blebs as described before (*15*). EL was induced by exposing the sample to a 180 μs electric field pulse of 0.7 kV/cm at 500 μs after a series of 1−12 saturating laser flashes. At this field strength PS I did not contribute significantly to the EL. Emitted light was collected on the photomultiplier. The photomultiplier signal was amplified (bandwidth >1 MHz), digitized at a sample frequency of 2 MHz, and fed into a PC for data averaging and storage. For each measurement a fresh dark-adapted sample was taken.

Data Analysis. Fits of the fluorescence were performed by relating the fraction of PS II centers with reduced Q_A^- (C) to the fluorescence according to Paillotin (*20*):

$$\frac{F}{F_M} = 1 - \frac{1 - C}{(1/\epsilon) - p(C)} \qquad (1)$$

F is the observed fluorescence yield. F_M is the fluorescence

yield corresponding to all centers closed ($C = 1$) by illumination in the presence of DCMU. $\epsilon = (F_M - F_0')/F_M$ is the trapping efficiency with all centers open ($C = 0$). The fluorescence yield in that case, F_0', is generally higher than the F_0 seen after dark adaptation, especially shortly after a flash, and hard to determine experimentally. For the value of F_0' we took the fitted value of the nondecaying (on a 1 s time scale) part of the fluorescence yield after the flash (see below), thus ignoring the presence of any Q_A^- in that. The connectivity parameter *p*, the probability of excitation transfer from a closed center to another PS II, was taken to be 0.7.

The oxidation of Q_A^- on the time scale of our measurements was modeled as the sum of two exponential decays with time constants τ_{fast} and τ_{slow}, and fractions of PS II centers involved Q_{fast} and Q_{slow}. Their sum Q_0 is less than 1; i.e., F_M is not reached, because in some centers charge recombination occurs before P_{680}^+ can be reduced by Y_Z. The first data point included in the fit was taken some time after the flash (typically 150 μs in the 10 ms experiments) to avoid contributions of rising phases in the fluorescence and/or instrument response. The presence of still slower phases in Q_A^- decay is ignored, resulting in an overestimation of F_0'. Least-squares fitting was performed using the routine e04jaf of the NAG toolbox for Matlab. This routine employs a quasi-Newton method to minimize a general nonlinear function and allows bounds to be imposed on the parameters. Confidence intervals of parameter values in the presence of cross-correlation between fit parameters were determined by a Monte Carlo fit simulation procedure (*21*) as used before (*15*). The method consists of first obtaining the most likely parameters by an ordinary least-squares fit of the real data. This fit is used to generate a large number of synthetic data sets by adding random noise with the same distribution as found in the original data. All synthetic data sets are then fitted in the same way as the original data to produce a distribution of values for each fit parameter. These distributions represent the confidence intervals including cross-correlations between the parameters.

RESULTS

To separate the effects of the two-electron gate from those of the four-step S-state cycle, chemicals that reduce the higher S-states between successive flashes in a series may be added. For this purpose so-called ADRY agents have often been used, because their presence in catalytic amounts destabilizes the higher S-states permanently (*22*, *23*). This is illustrated in Figure 1 by measurements of the recombination luminescence induced by a strong electric field pulse (EL) in osmotically swollen thylakoids. The integrated EL emitted during the first 100 μs of the pulse (for actual EL traces see the inset) is plotted as a function of the number of saturating flashes preceding the pulse, which was applied at 0.5 ms after the last flash. At this time the extent of Y_Z^{ox} reduction is very different in the different S-states, resulting in a strong flash number dependence of the EL amplitude with a characteristic periodicity of 4 flashes (triangles).

After addition of submicromolar concentrations of the ADRY agents CCCP (solid circles) or FCCP (open circles), the period four oscillation was completely suppressed. On all flashes the EL amplitude remained small, comparable to that observed after the first flash in the absence of ADRY agents. Apparently the S_2 state formed by the flash was reduced back to S_1 after each flash. The remaining flash number dependence indeed seems to show only a period two oscillation indicative of the two-electron gate at the electron acceptor side. However, two complications are clearly seen. First, the binary oscillation is not the same with the two ADRY agents: that with FCCP is barely resolved and its phase is opposite to that seen with CCCP. Second, the oscillation disappears in 8 flashes, indicating that the synchrony of the two-electron gate between PS II centers in the sample was lost much more quickly than the damping of the period four oscillation in the absence of ADRY agent would predict. The latter discrepancy could be quantified in first approximation by determination of the best-fitting miss probability if the period four oscillation was simulated by a simple Kok scheme with S-state independent misses, plus a small average EL increase per flash. This description is too simple to allow a good fit [as reported before (*24*)], but it showed that the average miss probability was between 5% and 8%, much lower than the 17.5% found when the EL oscillation with CCCP was simulated with a two-state model (solid lines in Figure 1).

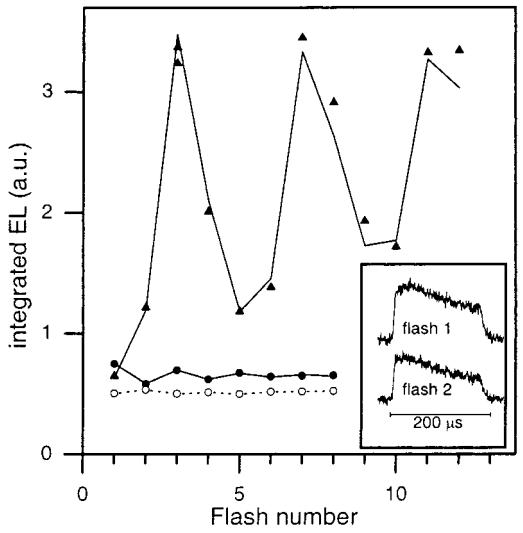

FIGURE 1: EL induced by a 0.7 kV/cm electric field pulse applied over a suspension of osmotically swollen chloroplasts (chlorophyll concentration 4 μg/mL). The field was switched on at 500 μs after a variable number of preceding laser flashes were fired at 1 Hz. Shown is the integrated EL yield from the first 100 μs of the electric field pulse as a function of flash number. Symbols: triangles, no additions; open circles, 0.1 μM FCCP; solid circles, 0.24 μM CCCP. The solid lines are fits as described in the text. The inset shows the actual EL transients after 1 and 2 flashes in the presence of CCCP.

The oxidation of Q_A^- after a flash is most conveniently monitored by the associated decrease of the chlorophyll fluorescence yield. Figure 2A shows the flash number dependence of fluorescence yield transients in thylakoids on a 0.2 ms (left) and on a 2 ms time scale (right), normalized to the fluorescence yield in the dark-adapted state. The maximum fluorescence, reached at about 50 μs after the flash, shows a period four oscillation with a flash number similar to those in refs *25*−*27*, attributed to an S-state dependent amount of long-lived P_{680}^+, which is a strong fluorescence quencher. The overall rise of the fluorescence yield with flash number results from depletion of the plastoquinone pool and could be completely prevented by the addition of 25 μM

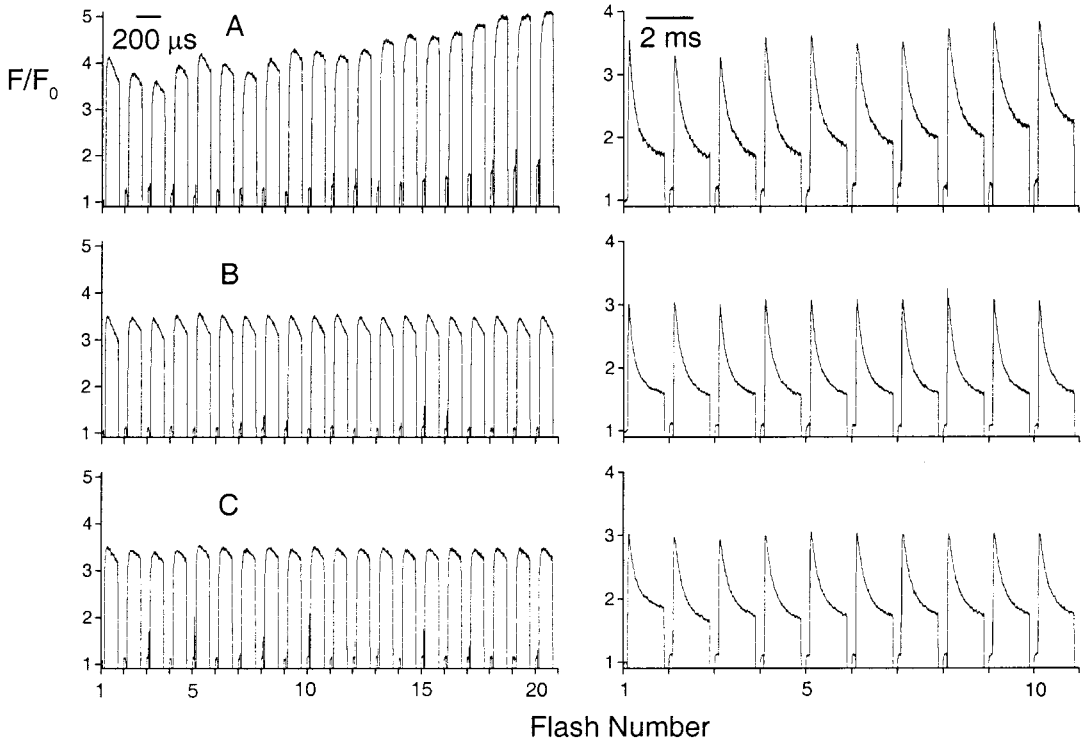

FIGURE 2: Flash-induced fluorescence changes induced by consecutive flashes fired at 1 Hz. Panels: left, 200 μs/transient; right, 2 ms/transient. Thylakoids were suspended at pH = 6.5; the chlorophyll concentration was 8 μg/mL. Conditions: (A) no additions; (B) 0.1 μM FCCP; (C) 0.24 μM CCCP.

artificial electron acceptor 2,5-dichloro-*p*-benzoquinone (not shown, but see ref *24*). When the ADRY agents FCCP (Figure 2B) or CCCP (Figure 2C) were added in sufficient amounts to suppress the period four oscillation, also the overall rise with flash number disappeared. This suggests that the reduction of the plastoquinone pool was prevented because the electrons reducing the higher S-states originate from the plastoquinone pool or PS II acceptor side.

As in the EL measurements, small period two oscillations of the flash-induced fluorescence changes appear in the presence of the ADRY agents, but they are not the same for CCCP and FCCP. In the presence of FCCP the initial fluorescence decay was accelerated and appeared to be faster on odd than on even flash numbers, at least for the first few flashes (Figure 2B, left). This was not observed with CCCP: here the most pronounced period two oscillation was observed in the fluorescence remaining after a few milliseconds (Figure 2C, right), which was larger than with FCCP or on the first four flashes without additions.

The overall impression from the 2 ms traces in Figure 2 is that the fluorescence yield decay kinetics after a flash shows little dependence on S-state or Q_B/Q_B^-. All traces show similar decay times. For quantitative analysis of the kinetics, the decay of the fluorescence yield after the first five flashes was measured on a 10 ms time scale (Figure 3). These traces show at least two decay components with time constants around 0.5 and 2 ms, respectively, and an offset (nondecaying on this 10 ms time scale but largely gone before the next flash, 1 s later; see Figure 2). In this and the following figures the dotted lines show the corresponding data obtained after replacement of H_2O by D_2O, which will be addressed at the end of the Results section.

Figure 4 shows the same data decomposed into the contributions of the four S-states, assuming the presence of 25% S_0 and 75% S_1 after dark adaptation and an S-state independent miss probability of 7.5% on each flash. Only the fluorescence yield transients on flash numbers 2−5 were used for the decomposition to avoid complications by the different contribution of "inactive centers" on first flash after dark adaptation, as compared to later flashes (*28*, *29*). The resulting traces show the fluorescence yield transient that would be seen if all active PS II centers were in the indicated S-state at the moment of the flash. Figures 2 and 3 already indicated the lower maximum in S_3, related to a larger $P_{680}^+Q_A^-$ recombination (*15*), and the lower offset after a flash in S_0, presumably because it forms neither Q_B^- nor a high S-state. The key result shown by the decomposition is the absence of the 2 ms component in Q_A^- oxidation after a flash fired in the states S_0 and S_2, where mainly Q_B^- is expected to be the electron acceptor.

A quantitative description was obtained by fitting the data of Figure 3. Kinetics of Q_A^- oxidation in each of the S-states were calculated according to the relevant parameters, mixed for each flash according to the S-state distribution calculated from the assumed dark distribution of S_0:S_1:S_2:S_3 = 0.25:0.75:0:0 and miss probability of 7.5% used in the construction of Figure 4, and converted to the fluorescence yield scale as described in Materials and Methods. It was assumed that the $S_1 \rightarrow S_2$ and $S_3 \rightarrow S_0$ transitions were associated with biexponential Q_A^- oxidation kinetics, while Q_A^- oxidation on the $S_0 \rightarrow S_1$ and $S_2 \rightarrow S_3$ transitions was assumed to be monoexponential. The fluorescence yield remaining after these decay phases was assumed to correspond to all Q_A oxidized, i.e., accounted for by F_0' (see Materials and Methods).

The smooth lines in Figure 3 represent the fit obtained as described above. Table 1 lists values of fit parameters corresponding to the hypothetical situation of a flash fired

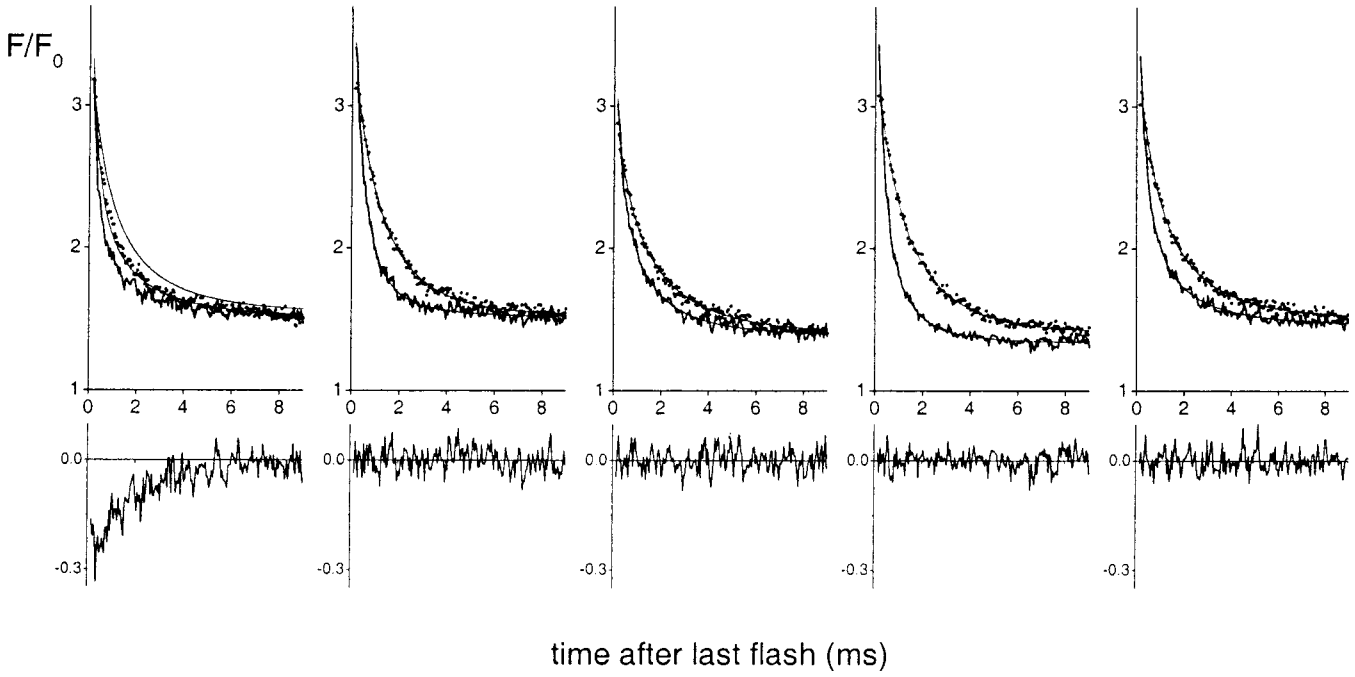

FIGURE 3: Time course of the fluorescence yield change during 9 ms after the last of 1−5 flashes fired at 1 Hz. Lines: solid, thylakoids suspended in H_2O; dotted, thylakoids suspended in D_2O (pH/D = 6.5). The smooth lines represent fits as described in the text. The residuals of the fit to the H_2O data are shown in the lower panels.

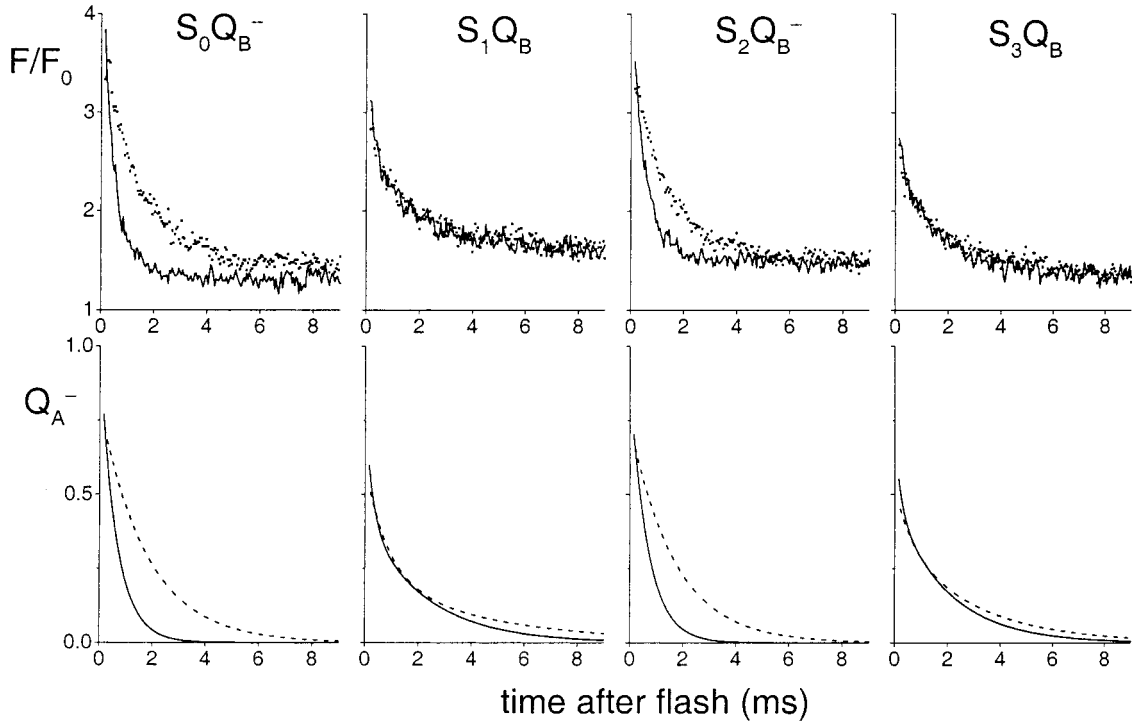

FIGURE 4: Upper panels: S-state decomposed fluorescence yield kinetics based on flashes 2−5 of the data in Figure 3. The transients represent the signal with all RCs in the indicated S-state just before the flash. Lines: solid, H_2O; dotted, D_2O. A miss probability of 0.075 in H_2O or 0.115 in D_2O and a dark distribution of S-states of S_0:S_1:S_2:S_3 = 0.25:0.75:0:0 were assumed for the decomposition. Lower panels: S-state decomposed decay kinetics of Q_A^- calculated according to the fit in Table 1. Lines: solid, H_2O, dotted, D_2O.

with 100% of the RCs in the indicated S/Q_B state. Corresponding Q_A^- decay kinetics calculated for each S-state transition are shown in Figure 4 (lower panels). It may be concluded that under the assumptions described above it is possible to describe the data in terms of a biphasic Q_B reduction and a monophasic Q_B^- reduction. This result does not depend much on the value of the miss probability used, but it does depend on the assumed presence of 20−30% $S_0Q_B^-$ in the dark. This is illustrated in Figure 5, which shows the mean square deviation between fit and data, normalized to the mean square noise, as a function of the fraction of centers assumed to have $S_0Q_B^-$ in the dark. A good fit was obtained for fractions of 0.25−0.3. For smaller fractions the overall mean square deviation seems small, but in parts of the signal, especially at short times after the second and the fourth flash, clearly significant deviations appeared. The

Table 1: Parameters Obtained by Fitting Flashes 2−5 of Figure 3 (pL 6.5) As Described in the Text[a]

	$S_0Q_B^-$		S_1Q_B		$S_2Q_B^-$		S_3Q_B	
	H_2O	D_2O	H_2O	D_2O	H_2O	D_2O	H_2O	D_2O
τ_{fast} (ms)	0.64	1.8	0.28	0.85	0.68	1.7	0.21	0.66
τ_{slow} (ms)			2.3	4.5			2.0	2.9
Q_0	0.95	0.78	0.75	0.57	0.85	0.72	0.70	0.50
Q_{fast}/Q_0	1 f	1 f	0.47	0.63	1 f	1 f	0.35	0.34
F_0'/F_0	1.32	1.43	1.58		1.49	1.48	1.34	

[a] Values apply when a flash is fired in the indicated S/Q_B state. Symbols are defined in Materials and Methods. f denotes a fixed parameter. Other fixed parameters are $F_{max} = 5.3$, $p = 0.7$, dark distribution of S-states $S_0:S_1:S_2:S_3 = 0.25:0.75:0:0$, and miss probability 7.5% in H_2O and 11.5% in D_2O (see ref *44*). For S_1 and S_3 the value of F_0' in D_2O was set to the same value as found in H_2O.

deviation on the first flash, which was disregarded in the minimization, shows that the 2 ms component on this flash is smaller than expected.

The fit results indicate that the rates of electron transfer from Q_A^- to Q_B and from Q_A^- to Q_B^- do not depend significantly on the S-state. Therefore, the decomposition of the decay of the fluorescence yield does not depend on the initial S-state distribution or correlation of S-state and Q_B-state that was assumed in the fit. The assumed presence of 25−30% Q_B^- in the dark is required and sufficient to conclude that the 2 ms component is not seen during Q_B^- reduction, which strongly supports its assignment to Q_A^- oxidation in centers where the Q_B site is empty at the moment of the flash. Its smaller amplitude on the first flash after dark adaptation may indicate that the 1 s flash interval was too short to reach plastoquinone binding equilibrium at the Q_B site in all centers.

The best-fitting time constants in Table 1 suggest that the rate of Q_B^- reduction is indeed slower than the fast phase of Q_B reduction, as was concluded by Bowes and Crofts (*14*). However, due to cross-correlation in the fit between the rate and amplitude of the fast component and the value of Q_0, this result was not unambiguous. A good fit could still be obtained when no Q_B/Q_B^- dependence of the time constant was allowed in the model, although the resulting flash number dependence of Q_0 appeared unlikely in view of the data at the shorter time scale in Figure 2. The ambiguity is no longer observed when ADRY agents are added to remove the S-state dependence of Q_0.

Figure 6 shows the flash-induced fluorescence yield transients in the presence of CCCP, measured on a 10 ms time scale as in Figure 3. As noted already in Figure 2, in the presence of CCCP the fluorescence yield remaining after a few milliseconss is higher than in the control or with FCCP and shows a rapidly damped but pronounced period two oscillation with flash number. A significant fraction of Q_A^- appears to be retained longer than the duration of measurement, especially on uneven flash numbers. Assuming that the oscillation is related to the two-electron gate, we can use it to decompose the kinetics into the contributions by electron transfer from Q_A^- to Q_B and that from Q_A^- to Q_B^-, respectively.

Any influence by the electron donor side should now be the same on each flash, except perhaps on the first where some $S_0 \rightarrow S_1$ is expected. The first flash was disregarded, and fitting was performed as above, but using a two-state

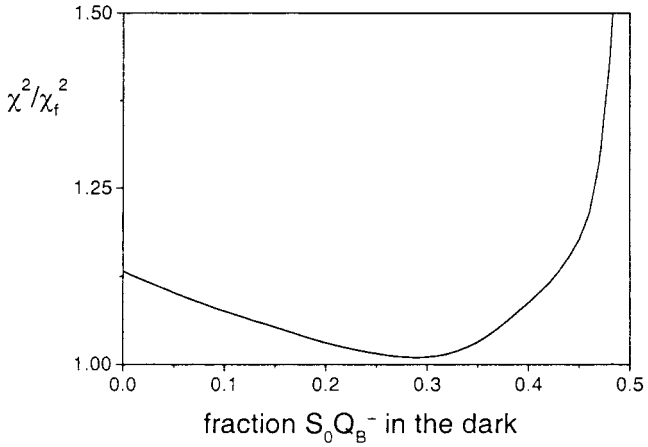

FIGURE 5: χ^2, the sum of squared residuals from a fit to the fluorescence yield transients in Figure 3 as described in the text, as a function of the fraction of $S_0Q_B^-$ assumed to be present in the dark. χ^2 is normalized to the mean square noise, χ_f^2.

model rather than a four-state model. F_0' and Q_0 can now be assumed to be the same for both Q_B and Q_B^- reduction. F_0' was assumed to correspond to the fluorescence left at 9 ms after Q_B^- reduction; the period two oscillation of this level was assumed to stem from Q_A^- retained after Q_B reduction (Q_{offset}). Again the 2 ms phase was assumed to occur only on Q_B reduction and not on Q_B^- reduction. The best-fitting parameter values are listed in Table 2 and the corresponding fluorescence yield kinetics shown by the smooth lines in Figure 6. The fit was sensitive to the miss probability, for which a similar value, 16%, was found as in the EL measurements of Figure 1. The fraction of Q_B^- assumed to be present in the dark-adapted state was less critical, with a broad optimum around 0.22. The best-fitting values for the time constant of the fast phase of Q_A^- oxidation were similar to those found in the absence of CCCP (Table 1): 0.24 ms for Q_B reduction and 0.79 ms for Q_B^- reduction.

The difference between the time constants of Q_B reduction and Q_B^- reduction was conclusive in this case, due to the more restrictive two-state model. The confidence distributions of the time constant of the fast phase of Q_A^- oxidation were determined by a Monte Carlo fit simulation as described in Materials and Methods and are shown in Figure 7. Given the best-fitting parameter valuess, the confidence distributions reflect the probability that the "real" values are different. Although without CCCP the confidence distributions for the time constants of Q_B (S_1Q_B, S_3Q_B) and Q_B^- ($S_0Q_B^-$, $S_2Q_B^-$) reduction are clearly different, they do overlap, and an acceptable fit could indeed be obtained assuming identical time constants for Q_B reduction and Q_B^- reduction. This is due to cross-correlation in the fit between the time constant of Q_B reduction, Q_0, and the relative amplitude of the 2 ms component. In the fits to the data with CCCP, the confidence distributions for the two time constants are widely separated, mainly because that for Q_B reduction is now sharply delimited. The reduction of Q_B^- may be somewhat slower in the presence of CCCP, but this effect was not significant.

The presence of a very slow phase in the reduction of Q_B is most easily explained by assuming that CCCP competes with plastoquinone for the Q_B binding pocket and, once bound, is not released within 10 ms. An interaction of CCCP with the PS II acceptor side similar to that of DCMU has

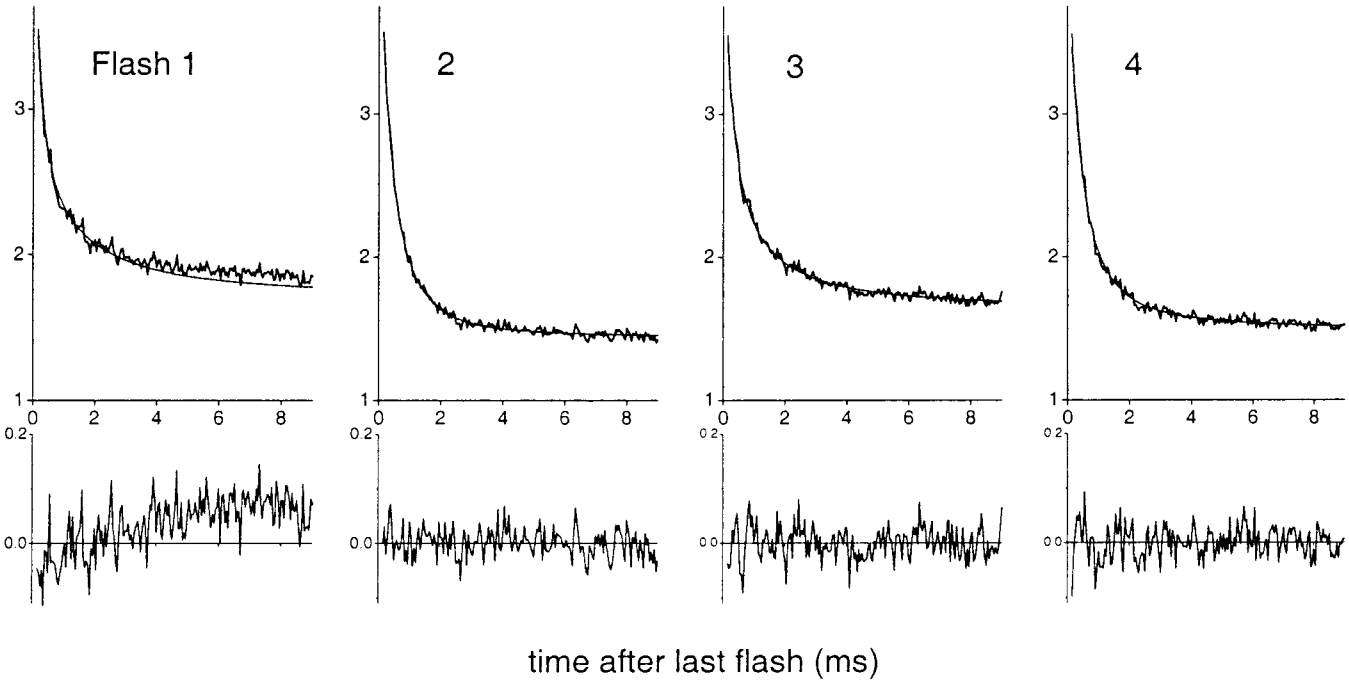

FIGURE 6: Time course of the flash-induced fluorescence change yield during 9 ms after the last of 1−4 flashes fired at 1 Hz in the presence of 0.5 μM CCCP. The solid lines represent fits as described in the text. The residuals to the fit are shown in the lower panels.

Table 2: Values of Parameters Found by Fitting the Data of Figure 6, Obtained in the Presence of CCCP (pH 6.5) As Described in the Text[a]

	S_1Q_B		$S_1Q_B^-$
τ_{fast} (ms)	0.24		0.79
τ_{slow} (ms)	2.8		
Q_0		0.95	
Q_{fast}/Q_0	0.38		1 f
Q_{slow}/Q_0	0.23		0 f
Q_{offset}/Q_0	0.38		0 f
F_0'/F_0		1.19	

[a] Values apply when a flash is fired in the indicated S/Q_B state. Symbols for fit parameters are defined in Materials and Methods. Q_{offset} denotes a fraction of Q_A^- that is left after the slow phase. Other parameters are miss probability 16% and fraction of Q_B^- present in the dark 0.22 in H_2O. f denotes a fixed parameter. Other fixed parameters are $F_{max} = 5.0$ and $p = 0.7$.

been suggested before (*11*, *30*). To verify this point, fluorescence yield changes induced by the addition of CCCP after flash illumination were measured (Figure 8). The thylakoids were dark adapted, and 25 μM electron donor TPB was added in the dark. Then the measuring light was switched on, and one flash was fired to produce Q_B^-. Subsequent addition of DCMU (dashed line) results in the expected fluorescence yield increase due to trapping of Q_A^- by the displacement of Q_B:

$$Q_AQ_B^- + DCMU \leftrightharpoons Q_A^-Q_B + DCMU \rightarrow Q_A^-DCMU + Q$$

After that, the fluorescence continues to increase slowly because of the now irreversible actinic effect of the measuring light. At the end of the trace a few flashes were fired to locate the F_M level. Addition of 0.24 μM CCCP before DCMU (solid line) caused a small increase by itself and diminished the increase induced by DCMU. At higher concentration FCCP caused similar effects (not shown), indicating that this ADRY agent also binds at the Q_B binding site but apparently not in significant amounts at the 0.1 μM concentration used in Figure 2.

Effects of pH and H_2O/D_2O Exchange on $Q_A \rightarrow Q_B$ Electron Transfer. Now that we can clearly distinguish the Q_A^- oxidation kinetics in PS II centers with Q_B, with Q_B^-, and with an empty Q_B site, it should be possible to determine the effects of pH and H_2O/D_2O exchange on each of these. In Figure 9 the flash-induced fluorescence changes measured at pL 5.5 and 7.8 are shown. At pH 5.5 the decay of Q_A^- is slower than at higher pH. Also, the H_2O/D_2O exchange effect is most pronounced at low pL. Fits of the data were performed in the same way as before and did not require unreasonable assumptions for the miss probability or dark distribution. The only complication was that on the $S_2 \rightarrow S_3$ transition in H_2O at pH 7.8 no fit could be obtained without allowing a slow phase. The significance of this disturbing observation is not clear. The results are presented in Table 3 and may be compared to those in Tables 1 and 2. The overall impression that emerges from these data is that all time constants may be increased by a factor of 2−3 by lowering the pL or by H_2O/D_2O exchange and no specific pattern can be distinguished in these effects. The amplitude of Q_0 is decreased, and in most cases that of F_0' is increased by D_2O. We note again that the fast and the slow phases of Q_B reduction (S_1, S_3) are hard to determine separately and their rates are correlated with Q_0 and the relative amplitude of the slow phase in the fit. As a result, especially the effects on the Q_B reduction kinetics suggested by the best-fitting parameter values may have limited significance. For instance, Figure 4 suggests that the data do not rule out the possibility that D_2O has no effect on Q_B reduction, in contrast to Q_B^- reduction. In D_2O at pD 5.5 the slow phase could no longer be distinguished, which explains the extra increase of F_0' on the S_{12} and S_{30} transitions in this case.

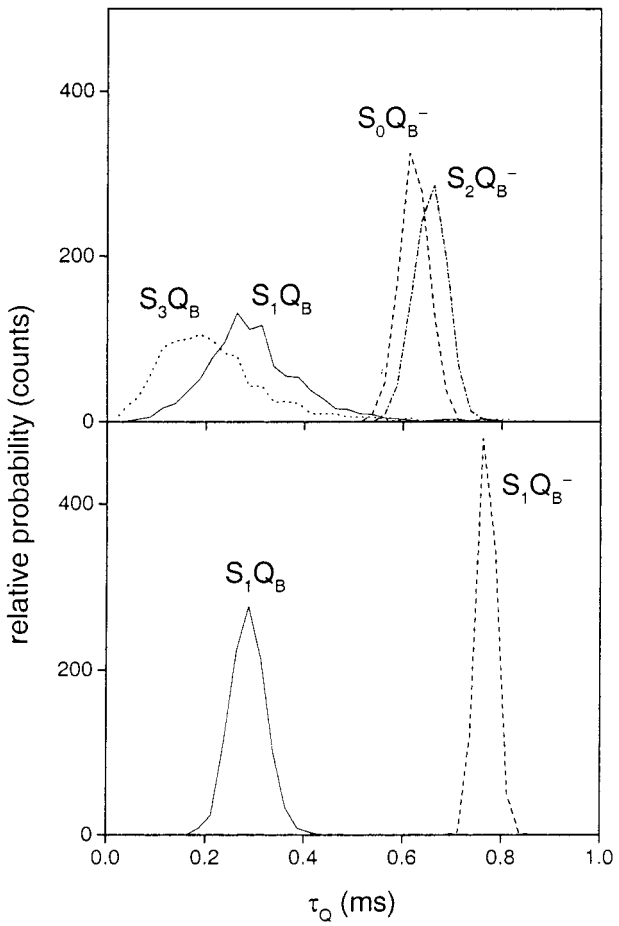

FIGURE 7: Confidence distributions for the value of the time constants of the fast phase of Q_A^- oxidation (τ_Q) within the model described in the text. The confidence distributions were obtained by a Monte Carlo simulation (see Materials and Methods). Upper panel: without additions (Figure 3), after a flash in $S_0Q_B^-$ (dashed line) and $S_2Q_B^-$ (dash-dotted line) or in S_1Q_B (solid line) and S_3Q_B (dotted line). Lower panel: in the presence of CCCP (Figure 6), Q_B reduction (solid line) or Q_B^- reduction (dashed line).

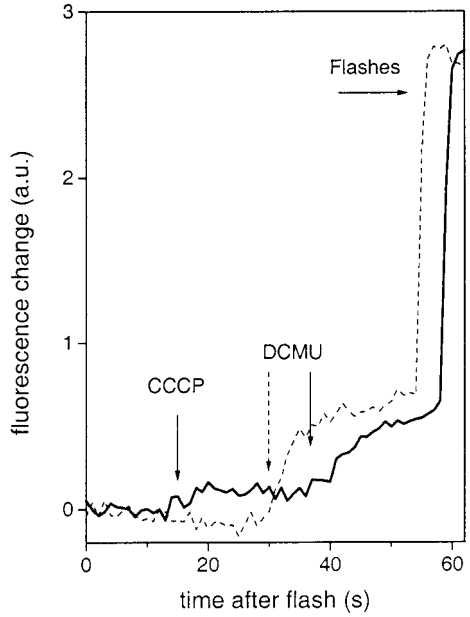

FIGURE 8: Fluorescence yield changes induced by the addition of chemicals. After dark adaptation 25 μM TPB and a flash was fired ($t = 0$). Lines: dashed, fluorescence change induced by the addition of 25 μM DCMU; solid, fluorescence changes induced by the successive addition of 0.24 μM CCCP and 25 μM DCMU.

DISCUSSION

The decay of the chlorophyll fluorescence yield in chloroplasts after a saturating flash is highly polyphasic. After approximate correction for the nonlinear dependence of fluorescence yield on the concentration of Q_A^-, mainly two kinetic components can be distinguished in the oxidation of Q_A^-, with time constants in the range of 0.2−0.8 and 2−3 ms, respectively, followed by a minor, much slower component. The time constants and amplitudes show small but reproducible oscillations with flash number, indicating a dependence on the S-state and Q_B-state. Determination of that dependence required decomposition of the data into the contributions of each state to the mixture present in the sample, because the differences are too small to distinguish these contributions in a mixed decay curve.

S-State/Q_B-State Decomposition. This decomposition requires knowledge of the initial distribution of states and of their transition probabilities in a flash. The simplifying assumption of state-independent misses is usually a satisfactory approximation for this purpose, and the average transition probability is easily determined from the damping of any parameter modulated by the oscillation. The distribution of states after 15 min dark adaptation is uncertain. Deactivation of the higher S-states would be expected to proceed most rapidly via back-reaction with Q_B^-, if present. In a sample with random distribution of S-states and Q_B^--states, that would produce a distribution of $^1/_8$ S_0Q_B, $^1/_8$ $S_0Q_B^-$, $^5/_8$ S_1Q_B, and $^1/_8$ $S_1Q_B^-$ after dark adaptation. Both S_0 and Q_B^- will be present in one-fourth of the centers, but coexist in one-eigthth only. In the fits of Tables 1 and 3 they were kept strictly correlated, to make use of the constraint of monophasic Q_B^- reduction, and as a result the initial S_0 concentration may be overestimated. Such a strict correlation was actually found in the—to our knowledge—only published attempt to measure it (*11*), but there the dark distribution was 0.1 $S_0Q_B^-$, 0.9 S_1Q_B, possibly related to the long dark adaptation used. The presence of some 30% Q_B^- in the dark has been postulated before (*7*, *31*) but is not well established (*24*). We show here that the assumption of 25−30% Q_B^- after dark adaptation is required and sufficient to conclude that the 2−3 ms phase in Q_A^- oxidation probably does not occur on Q_B^- reduction but only on Q_B reduction, as expected if it reflects plastoquinone binding to an empty Q_B site.

CCCP and Plastoquinol. Despite the constraints imposed by the assumed restriction of Q_B^- to even and Q_B to uneven S-states and a monophasic Q_B^- reduction and biphasic Q_B reduction, there were too many free parameters to prove the apparent rate difference between these two reductions. Especially the time constant of the fast phase of Q_B reduction was poorly defined due to cross-correlation between the amplitudes and time constants of the two phases. The required simplification was obtained by adding the ADRY agent CCCP to remove all S-state dependence, especially of Q_0 and F_0', because CCCP also caused a binary oscillation of the fluorescence yield at 10 ms that could be used for Q_B/Q_B^- decomposition of the data. The oscillation was due to a very slow phase (~0.1 s) in Q_A^- oxidation which we attribute to the displacement of CCCP from the Q_B site by plastoquinone after photoreduction of Q_A. Recombination of

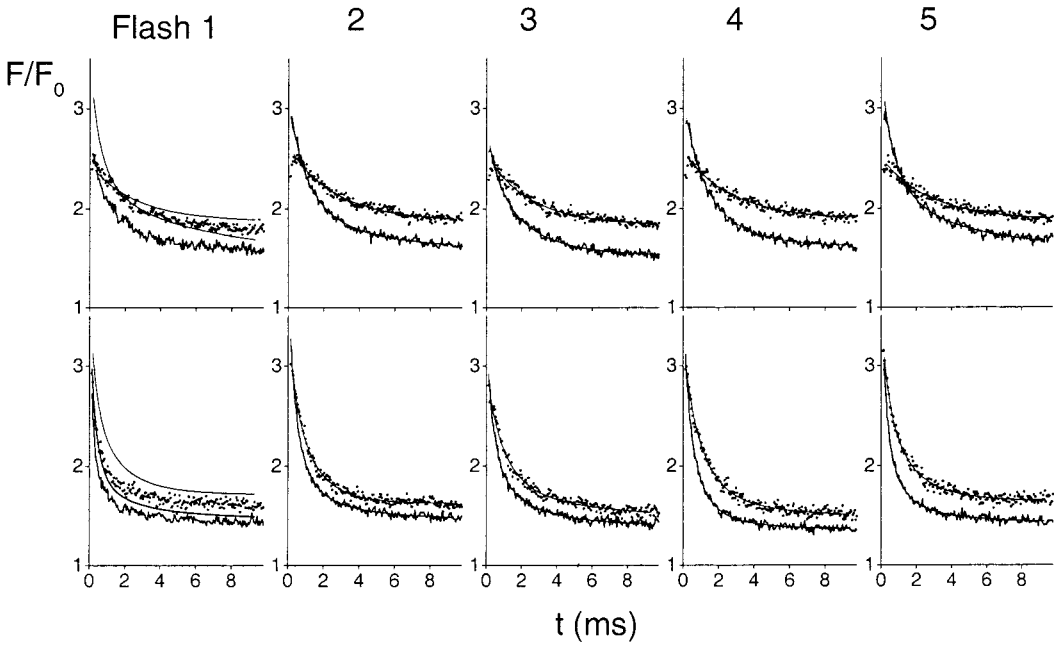

FIGURE 9: Flash-induced fluorescence yield change induced by the last of 1−5 flashes (as in Figure 3) in H_2O (solid experimental lines) and D_2O (dotted lines) at pL (pH, pD) 5.5 (upper panels) and 7.8 (lower panels). The smooth lines are fits as described in the text.

this long-lived Q_A^- with the S_2 state, before the ADRY effect has reduced S_2 to S_1, may explain the enhanced miss probability in the binary oscillation.

It seems that plastoquinol has a similar effect: the fluorescence yield remaining after 2 ms was found to increase much earlier during the flash series than that remaining after 1 s, just before the next flash (Figure 2, upper frame). The increase is too large to be due to decreased fluorescence quenching by plastoquinone. By analogy to the effect of CCCP, we attribute this increasing slow (>10 ms) phase in the fluorescence yield decay to the dissociation of plastoquinol from the Q_B site in response to the much stronger binding of Q_B^-.

The small fluorescence yield decay phase in the 10 ms to 1 s time range present already on the first few flashes, also seen in the presence of FCCP, presumably has a different origin. Its association with Q_A^- oxidation or a change in trapping efficiency and possible connection to PS II heterogeneity is not clear (*16*, *32*). The existence of so-called "non-B" centers (*33*) is not apparent from our data. If they do contribute to the flash-induced fluorescence yield transients, it would have to be in this small, very slow component contained in F_0'.

The ADRY agents prevented the accumulation of plastoquinol during the flash series but not the functioning of the two-electron gate, supporting earlier evidence that the electrons reducing the high S-states are ultimately derived from the plastoquinone pool (*34*, *35*). This may seem inconsistent with the persistence of the ADRY effect in the presence of DCMU under repetitive flash conditions in the presence of divalent cations and a high concentration of ferricyanide (*36*). However, in such conditions ferricyanide probably mediates electron transfer from Q_A^- to the oxidized ADRY agent.

Time Constants of Electron Transfer from Q_A^- to Q_B and to Q_B^-. The fluorescence yield transients in the presence of CCCP show time constants for the reduction of Q_B and that of Q_B^- of 0.2−0.4 and 0.7−0.8 ms, respectively (Figure 7).

Table 3: Fit Parameters Found by Fitting Flashes 2−5 of the Flash-Induced Fluorescence Yield Kinetics in Thylakoids at pL (pH, pD) 5.5 and 7.8 in H_2O and D_2O (Figure 9) As Described in the Text[a]

	$S_0Q_B^-$		S_1Q_B		$S_2Q_B^-$		S_3Q_B	
	H_2O	D_2O	H_2O	D_2O	H_2O	D_2O	H_2O	D_2O
				pL = 5.5				
τ_{fast} (ms)	1.8	3.8	0.9	2.6	1.7	3.2	1.4	2.5
τ_{slow} (ms)			9.9				5.6	
Q_0	0.69	0.35	0.61	0.27	0.62	0.41	0.46	0.32
Q_{fast}/Q_0	1 f	1 f	0.42	1 f	1 f	1 f	0.60	1 f
F_0'/F_0	1.72	1.94	1.40	1.84	1.61	1.87	1.41	1.79
				pL = 7.8				
τ_{fast} (ms)	0.83	1.4	0.32	0.70	0.73	1.3	0.35	1.1
τ_{slow} (ms)			3.3	3.1	2.7		2.6	7.0
Q_0	0.85	0.75	0.76	0.65	0.85	0.69	0.6	0.55
Q_{fast}/Q_0	1 f	1 f	0.71	0.68	0.75	1 f	0.54	0.51
F_0'/F_0	1.34	1.51	1.52	1.78	1.45	1.55	1.36	1.36

[a] Values apply when a flash is fired in the indicated S/Q_B state. At pL 7.8, the miss probability is 12% in H_2O and 10.5% in D_2O. At pL 5.5, the miss probability $m = 10\%$ in H_2O and 13.5% in D_2O (see ref *44*). The S-state distribution after dark adaptation was assumed to be $S_0:S_1:S_2:S_3 = 0.25:0.75:0:0$. f denotes a fixed parameter. Other fixed parameters are $F_{max} = 5$ and $p = 0.7$. Symbols for fit parameters are defined in Materials and Methods.

No significant S-state dependence was found, because these times are consistent with the fit result based on flash numbers 2−5 under oxygen-evolving conditions (Table 1). They are also consistent with the values based on the fluorescence yield decay after the first and second flash by Bowes and Crofts (*14*). PS II measurements on the first flash often differ from those during the rest of the flash series, but the time constant of electron transfer from Q_A^- to Q_B is the same. The fluorescence yield transient on the first flash after dark adaptation deviates from the fit based on flash numbers 2−5 mainly by the smaller amplitude of the 2−3 ms component (Figure 3). This component presumably reflects the equilibration of plastoquinone binding at the Q_B site with the locally available pool only. The high density of protein

complexes in the thylakoid membrane fragments the lipid space available for plastoquinone diffusion, and the number of plastoquinone molecules rapidly accessible to a PS II center can be quite small (*24*, *37*, *38*). The local concentration may decrease significantly with each molecule reduced during the flash series. A redistribution time of plastoquinone between local pools of 9 s has been reported (*37*), and that between PS II-rich membrane regions and PS I-rich regions could be even slower.

Protons. The reduction of quinone to quinol involves the binding of two protons, presumably under rather different circumstances, and the binding of plastoquinone to an empty Q_B site presumably does not. Yet the 2−3-fold retardation of Q_A^- oxidation by lowering the pH from 6.5 to 5.5 or H_2O/D_2O exchange did not allow us to detect a significant dependence of this effect on the occupancy of the Q_B site by Q_B, Q_B^-, or neither of the two. The retardation of Q_B reduction may be explained by a slower relaxation toward the equilibrium between $Q_A^-Q_B$ and $Q_AQ_B^-$ and/or a smaller fraction of bound Q_B (*39*, *40*); our data do not allow an unambiguous decomposition in this case. A slower fluorescence decay after H_2O/D_2O exchange was previously reported (*15*, *41*). It appears that a significant isotope exchange effect occurs on the rate of both Q_B and Q_B^- reduction, although that on Q_B reduction may not be significant. Apparently, these effects are quite indirect and influence the electron-transfer kinetics only via the ensemble of protonation equilibria of the surrounding protein. Presumably the binding, reduction, and dissociation of plastoquinone are all accompanied by shifts in an extensive network of hydrogen bonds in the protein similar to that in purple bacteria (*4*).

CONCLUDING REMARKS

Bowes and Crofts (*14*) originally proposed a faster rate of Q_B reduction than of Q_B^- reduction. We confirm this difference (Figure 7) (at pH 6.5) and show that it also applies after flash 2−5 and not only for the difference between flash 1 and flash 2 considered by Bowes and Crofts (pH 7.8). However, a scheme may be applied in which the overall decay is actually slower for Q_B reduction, due to the presence of a slow decay phase that does not occur on Q_B^- reduction (Figure 4). This slow phase has a relatively low amplitude on the first flash compared to the third and fifth flash, which is why the difference in Q_B/Q_B^- reduction kinetics is relatively easily observed by comparison of the first and second flash.

It is still unclear if a conformational rearrangement as in purple bacteria, which shifts Q_B from a "distal", inactive to a "proximal", active position (*12*), plays a role in PS II as suggested in ref *42*. In reaction centers isolated from purple bacteria, this conformational change is likely limiting the Q_B reduction rate (*6*). If the 2−3 ms component in PS II were due to such a process, we would have to assume that Q_B is already in the proximal site before the flash in a large fraction of the centers. Moreover, the Q_B and Q_B^- reduction times in bacterial reaction centers are 0.1 and 1 ms, respectively (*6*), similar to the fast phase in PS II, and in chromatophores these times may be even shorter, especially at low pH (*43*).

The 2−3 ms phase in $Q_A^- \rightarrow Q_B$ electron transfer has often been assumed to result from Q_B binding in centers with an empty binding site. We show that the occurrence of this phase may indeed be associated exclusively with Q_B reduction and not with Q_B^- reduction. This scheme offers an attractive description of the decay kinetics of Q_A^- in the first 10 ms after the charge separation. The period two modulation of the relative amplitude of the slow phase results naturally from the difference in PS II binding affinity of Q_B and Q_B^-. No heterogeneity of active and inactive PS II, let alone a dependence of the fraction of inactive (in oxygen evolution) centers on the redox state of Q_B, needs to be assumed (*16*).

ACKNOWLEDGMENT

We thank Drs. I. Vass, M. Okamura, and B. A. Diner for helpful advice.

REFERENCES

1. Diner, B. A., and Babcock, G. T. (1996) in *Oxygenic Photosynthesis: The Light Reactions* (Ort, D. R., and Yocum, C. F., Eds.) pp 213−247, Kluwer Academic Publishers, Dordrecht.
2. Schilstra, M. J., Rappaport, F., Nugent, J. H. A., Barnett, C. J., and Klug, D. R. (1998) *Biochemistry 37*, 3974−3981.
3. Tommos, C., and Babcock, G. T. (2000) *Biochim. Biophys. Acta 1458*, 199−219.
4. Diner, B. A., Petrouleas, V., and Wendoloski, J. J. (1991) *Physiol. Plant. 81*, 423−436.
5. Okamura, M., and Feher, G. (1995) in *Anoxygenic Photosynthetic Bacteria* (Blankenship, R. E., Madigan, M. T., and Bauer, C. E., Eds.) pp 577−594, Kluwer Academic Publishers, Dordrecht.
6. Okamura, M., Paddock, M. L., Graige, M. S., and Feher, G. (2000) *Biochim. Biophys. Acta 1458*, 148−163.
7. Bouges-Bocquet, B. (1973) *Biochim. Biophys. Acta 314*, 250−256.
8. Velthuys, B. R., and Amesz, J. (1974) *Biochim. Biophys. Acta 333*, 85−94.
9. Velthuys, B. R. (1981) *FEBS Lett. 126*, 277−281.
10. Velthuys, B. R. (1982) in *Function of Quinones in Energy Conserving Systems* (Trumpower, B. L., Ed.) pp 401−408, Academic Press, New York.
11. Van Gorkom, H. J., Thielen, A. P. G. M., and Gorren, A. C. F. (1982) in *Function of Quinones in Energy Conserving Systems* (Trumpower, B. L., Ed.) pp 213−225, Academic Press, New York.
12. Stowell, M. H. B., McPhillips, T. M., Rees, D. C., Soltis, S. M., Abresch, E., and Feher, G. (1997) *Science 276*, 812−816.
13. Van Gorkom, H. J. (1986) in *Light Emission by Plants and Bacteria* (Govindjee, C. A., Amesz, J., and Fork, D. C., Eds.) pp 267−289, Academic Press, Orlando, FL.
14. Bowes, J. M., and Crofts, A. R. (1980) *Biochim. Biophys. Acta 590*, 373−384.
15. De Wijn, R., Schrama, T., and van Gorkom, H. J. (2001) *Biochemistry 40*, 5821−5834.
16. Putrenko, I. I., Vasil'ev, S., and Bruce, D. (1999) *Biochemistry 38*, 10632−10641.
17. Robinson, H. H., and Yocum, C. F. (1980) *Biochim. Biophys. Acta 590*, 97−106.
18. Schowen, R. L. (1977) in *Isotope Effects on Enzyme-Catalyzed Reactions* (Cleland, W. W., O'Leary, M. H., and Northrop, D. B., Eds.) pp 64−99, University Park Press, Baltimore, MD.
19. Herman, J. R., Londo, T. R., Rahman, N. A., and Barisas, B. G. (1992) *Rev. Sci. Instrum. 63*, 5454−5458.
20. Paillotin, G. (1976) *J. Theor. Biol. 58*, 237−252.
21. Straume, M., and Johnson, L. J. (1992) in *Methods in Enzymology, Volume 210: Numerical Computer Methods* (Brand, L., and Johnson, L. J., Eds.) pp 117−129, Academic Press, New York.
22. Crofts, A. R., and Wraight, C. A. (1983) *Biochim. Biophys. Acta 726*, 149−185.
23. Renger, G. (1972) *Eur. J. Biochem 27*, 259−269.

24. Hemelrijk, P. W., and van Gorkom, H. J. (1996) *Biochim. Biophys. Acta 1274*, 31−38.
25. Christen, G., and Renger, G. (1999) *Biochemistry 38*, 2068−2077.
26. Shinkarev, V. P., Xu, C., Govindjee, C. A., and Wraight, C. A. (1997) *Photosynth. Res. 51*, 43−49.
27. Zankel, K. L. (1973) *Biochim. Biophys. Acta 325*, 138−148.
28. Dekker, J. P., van Gorkom, H. J., Wensink, J., and Ouwehand, L. (1984) *Biochim. Biophys. Acta 767*, 1−9.
29. Lavergne, J., and Leci, E. (1993) *Photosynth. Res. 35*, 323−343.
30. Homann, P. H. (1972) *Eur. J. Biochem 33*, 247−252.
31. Fowler, C. F. (1977) *Biochim. Biophys. Acta 459*, 351−361.
32. Diner, B. A., and Joliot, P. (1976) *Biochim. Biophys. Acta 423*, 479−498.
33. Lavergne, J., and Briantais, J. M. (1966) in *Oxygenic Photosynthesis: The Light Reactions* (Ort, D. R., and Yocum, C. F., Eds.) pp 265−287, Kluwer Academic Publishers, Dordrecht.
34. McCauley, S. W., Melis, A., Tang, G. M. S., and Arnon, D. I. (1987) *Proc. Natl. Acad. Sci. U.S.A. 84*, 8424−8428.
35. Samuilov, V. D., Renger, G., Paschenko, V. Z., Oleskin, A. V., Gusev, M. V., Gubanova, O. N., Vasil'ev, S., and Barsky, E. L. (1995) *Photosynth. Res. 46*, 455−465.
36. Ghanotakis, D. F., Yerkes, C. T., and Babcock, G. T. (1982) *Biochim. Biophys. Acta 682*, 21−31.
37. Joliot, P., Lavergne, J., and Beal, D. (1992) *Biochim. Biophys. Acta 1101*, 1−12.
38. Lavergne, J., Bouchaud, J. P., and Joliot, P. (1992) *Biochim. Biophys. Acta 1101*, *13*−22.
39. Robinson, H. H., and Crofts, A. R. (1984) in *Advances in Photosynthesis Research* (Sybesma, C., Ed.) pp 477−480, Martinus Nijhoff/Dr. W. Junk Publishers, The Hague, Boston, and Lancaster.
40. Taoka, S., and Crofts, A. R. (1989) in *Current Research in Photosynthesis* (Baltscheffsky, M., Ed.) pp 547−550, Kluwer Academic Publishers, Dordrecht.
41. Renger, G., Eckert, H. J., Bergmann, A., Bernarding, J., Liu, B., Napiwotzki, A., Reifarth, F., and Eichler, H. J. (1995) *Aust. J. Plant. Physiol. 22*, 167−181.
42. Garbers, A., Reifarth, F., Kurreck, J., Renger, G., and Parak, F. (1998) *Biochemistry 37*, 11399−11404.
43. Vermeglio, A. (1982) in *Function of Quinones in Energy Conserving Systems* (Trumpower, B. L., Ed.) pp 169−180, Academic Press, New York.
44. Christen, G., Seeliger, A., and Renger, G. (1999) *Biochemistry 38*, 6082−6092.

BI010852R